Radiochim. Acta **101**, 625–630 (2013) / **DOI** 10.1524/ract.2013.2085

Substitution of IO_3^-, IO_4^-, SeO_3^{2-}, and SeO_4^{2-} for CO_3^{2-} in $Na_4[UO_2(CO_3)_3]$

By S. Wu[1,2], F. Chen[1,*], A. Simonetti[2] and T. E. Albrecht-Schmitt[3,*]

[1] Guangzhou Institute of Geochemistry, Chinese Academy of Sciences, Guangzhou, Guangdong, 510640, China
[2] Department of Civil Engineering and Geological Sciences and Department of Chemistry and Biochemistry, University of Notre Dame, Notre Dame, Indiana, 46556, USA
[3] Department of Chemistry and Biochemistry, Florida State University, Tallahassee, Florida, 32306-4390, USA

(Received 1 November 2011; accepted in revised form April 26, 2013)
(Published online October 7, 2013)

Substitution / Iodine / Selenium / Uranyl carbonate

Summary. Trigonal sodium uranyl carbonate, $Na_4[UO_2(CO_3)_3]$, has been synthesized under hydrothermal conditions, and its incorporation of IO_3^-, IO_4^-, SeO_3^{2-}, and SeO_4^{2-} has been investigated. LA-ICP-MS was used to detect the presence and concentration of iodine, selenium, and uranium in single crystals of $Na_4[UO_2(CO_3)_3]$, and these in-situ analyses indicate that IO_3^-, IO_4^-, SeO_3^{2-}, and SeO_4^{2-} have been incorporated into its structure. The proposed mechanisms are the substitution of IO_3^-, IO_4^-, SeO_3^{2-}, and SeO_4^{2-} for CO_3^{2-}. The incorporation of iodine oxoanions results in the loss of Na^+ cations so as to maintain charge balance; the substitution schemes may be expressed as follows: $\square + IO_3^- \leftrightarrow Na^+ + CO_3^{2-}$ and $\square + IO_4^- \leftrightarrow Na^+ + CO_3^{2-}$ ($\square$ = vacancy).

1. Introduction

Carbonate, CO_3^{2-}, is one of the dominant and ubiquitous anions present within the natural aqueous environment. Once the uranyl ion, UO_2^{2+}, is released into an aqueous system, a series of UO_2^{2+}-CO_3^{2-} species form. Within these species, $[UO_2(CO_3)_3]^{4-}$ is one of the most stable and exists within a wide range of pH values from 6.5 to 11.5 [1]. Because of its stability and high solubility, $[UO_2(CO_3)_3]^{4-}$ is widely used to leach uranium from minerals in the uranium mining industry. The potential for aquatic transport of uranium as a result of carbonate complexation is reflected in the formation of naturally occurring uranyl carbonate minerals [2] such as rutherfordine, UO_2CO_3 [3], wyartite, $Ca[U(UO_2)_2(CO_3)O_4(OH)]\cdot 18H_2O$ [4], and čejkaite, $Na_4[UO_2(CO_3)_3]$ [5]. Within the known 45 uranyl carbonate minerals and inorganic compounds, 24 of them contain the $[UO_2(CO_3)_3]^{4-}$ anion. As shown in Fig. 1, a uranyl ion, UO_2^{2+}, is coordinated by three CO_3^{2-} in $[UO_2(CO_3)_3]^{4-}$. Cations, such as Li^+, Na^+, Ca^{2+}, and Mg^{2+}, form coulombic interactions with the $[UO_2(CO_3)_3]^{4-}$ anions and yield stable minerals or compounds which have the general formula of $M^+_xM'^{2+}_y[UO_2(CO_3)_3]\cdot nH_2O$ ($x = 0$–4, $y = 0$–2, $x + 2y \leq 4$).

Čejkaite is a triclinic uranyl carbonate mineral found in Jáchymov, Czech Republic [5–7] and the detailed structure has been described by Ondruš *et al.* [5]. A trigonal polymorph of Čejkaite, $Na_4[UO_2(CO_3)_3]$, has also been synthesized and reported [8–11]. Ondruš *et al.* found that under hydrothermal conditions at about 200 °C, čejkaite will recrystallize to trigonal $Na_4[UO_2(CO_3)_3]$ [5]. The basic structural motif of the $[UO_2(CO_3)_3]^{4-}$ anion is observed both in čejkaite and trigonal $Na_4[UO_2(CO_3)_3]$.

Both selenium and iodine are essential nutrients to humans and are related to some important physiologic roles and diseases [12]. Many fission products, including ^{79}Se (half life: 2.95×10^5 y) and ^{129}I (half life: 1.57×10^7 y), will be generated during nuclear fission, especially in nuclear reactors. Based on the performance assessments at Yucca Mountain and other proposed repositories, both ^{79}Se and ^{129}I are within the limited number of long-lived radionuclides that make the dominant contributions to final dose calculations [13, 14]. Once ^{79}Se and ^{129}I are released from the repositories, it will be potentially hazardous to humans and animals. Therefore, the geological behavior, such as adsorption, distribution, and migration of ^{79}Se [15–19] and ^{129}I [20–26] are important and well investigated.

Chen *et al.* [27] predicted the possibility that selenium would be incorporated into the alteration uranyl phases in trace quantity in the form of SeO_3^{2-} and SeO_4^{2-}, which is a potential mechanism for the immobilization of selenium. Our previous studies have demonstrated that ^{129}I can be incorporated into a uranyl silicate and phosphate in the form of iodate [28–30]. However, the possibility of iodate incorporation into other uranyl minerals and compounds, such as uranyl carbonate, is still unknown. However, the substitution of $PO_4^{3-} \leftrightarrow CO_3^{2-}$ is well established in apatite [31–33], and the substitutions of $SeO_3^{2-} \leftrightarrow CO_3^{2-}$ and $SeO_4^{2-} \leftrightarrow CO_3^{2-}$ in calcite have also been reported [34–37]. Considering the similar geometries of rutherfordine, UO_2CO_3, and UO_2SeO_3, Chen *et al.* predicted that SeO_3^{2-} will substitute for CO_3^{2-} in rutherfordine [27]. Unfortunately, there is no experimental evidence for this prediction until this study. Therefore, the incorporation of IO_3^-, IO_4^-,

*Authors for correspondence
(E-mail: frchen@gig.ac.cn, albrecht-schmitt@chem.fsu.edu).

SeO_3^{2-} and SeO_4^{2-} into the trigonal $Na_4[UO_2(CO_3)_3]$, a typical model of uranyl carbonate, was investigated and the possible substitution mechanisms are also discussed.

2. Experimental section

2.1 Syntheses

0.2009 g of $UO_2(NO_3)_3 \cdot 6H_2O$ (0.4 mmol), 0.085 g Na_2CO_3 (0.8 mmol) and 0.5 mL of H_2O were loaded in a 23 mL PTFE-lined autoclave. The autoclave was sealed and heated in a furnace at 180 °C for 3 d. The furnace was then cooled at 9 °C/h to room temperature. The product was washed with water and ethanol and allowed to dry. The produce consisted of yellow prism crystals and a yellow powder of $Na_4[UO_2(CO_3)_3]$. *While the $UO_2(NO_3)_2{\cdot}2H_2O$ used in this study contained depleted U, standard precautions for handling radioactive materials should be followed.*

2.2 Incorporation of iodine and selenium

In order to compare iodine and selenium uptake by crystals grown in the presence of iodine and selenium *vs.* those grown in the absence of iodine and selenium, but added back into iodine and selenium solutions, two group of experiments were designed as follows: (1) $Na_4[UO_2(CO_3)_3]$ was synthesized in the presence of HIO_3, H_5IO_6, SeO_2 or Na_2SeO_4, respectively. Samples were labeled as **NaUCI1a**, **NaUCI1b** (HIO_3), **NaUCI2a**, **NaUCI2b** (H_5IO_6), **NaUCSe1a**, **NaUCSe1b** (SeO_2), **NaUCSe2a** and **NaUCSe2b** (Na_2SeO_4), respectively. (2) 0.2168 g of synthesized iodine/selenium-free $Na_4[UO_2(CO_3)_3]$, and 0.5 mL of H_2O were reacted with HIO_3, H_5IO_6, SeO_2, or Na_2SeO_4 at 180 °C for 3 d. Samples were labeled as **NaUCI1c**, **NaUCI1d** (HIO_3), **NaUCI2c**, **NaUCI2d** (H_5IO_6), **NaUCSe1c**, **NaUCSe1d** (SeO_2), **NaUCSe2c**, and **NaUCSe2d** (Na_2SeO_4), respectively. Other procedures are the same as for the synthesis of $Na_4[UO_2(CO_3)_3]$. The ratios of uranium to iodine or selenium in all reactions were kept as 20 : 1 (a, c) and 10 : 1 (b, d). Natural abundance selenium and ^{127}I were used in the experiments.

2.3 Crystallographic studies

Unit cells of single crystals of iodine/selenium-free and iodine/selenium-bearing $Na_4[UO_2(CO_3)_3]$ were determined using a Bruker SMART APEX CCD X-ray diffractometer.

2.4 Laser-ablation inductively coupled plasma mass spectrometer (LA-ICP-MS) analysis

The iodine, selenium, and uranium content of the experimental products were investigated using a ThermoFinnigan high resolution magnetic sector Element2 ICP-MS instrument coupled to a UP213 Nd:YAG laser ablation system (New Wave Research). The method has been described elsewhere [30]. ^{78}Se, ^{127}I and ^{235}U ion signals were measured and total selenium and uranium contents were calculated according to the abundance of ^{78}Se in natural selenium (0.2377) and ^{235}U in depleted uranium (0.036). Based on the stoichiometric U content in $Na_4[UO_2(CO_3)_3]$, the iodine and selenium concentrations were estimated using the calculated I/U and Se/U ratios based on the measured ion signals of the respective elements (isotopes).

2.5 Thermal gravimetric analysis (TGA)

TGA measurements of typical samples were conducted using a Netzsch TG209F1 Iris thermal analyzer. 1.5–13 mg single crystals were selected under microscope and ground to powder. Subsequently, these were loaded into an aluminum crucible and heated from 20 to 900 °C at a rate of 5 °C/min within a stream of nitrogen gas.

3. Results and discussion

3.1 Structure of trigonal $Na_4[UO_2(CO_3)_3]$

The uranyl ion, UO_2^{2+}, is coordinated by three CO_3^{2-} anions to form uranyl tricarbonate anion, $[UO_2(CO_3)_3]^{4-}$, which is shown in Fig. 1. There are three crystallographically unqiue Na^+ cations in $Na_4[UO_2(CO_3)_3]$. Na(1) and Na(2) are octahedrally coordinated by six O atoms to form NaO_6 polyhedron and Na(3) is coordinated by five O atoms to form NaO_5 polyhedron (Figs. S1a, S1b). Na(1)O_6 octahedron is connected to adjacent Na(2)O_6 octahedron by face sharing to form a chain of alternating polyhedra around Na(1) and Na(2) along the *c* axis. Each Na(3)O_5 polyhedron is connected to other two Na(3)O_5 polyhedron *via* edge sharing to form a cluster containing three Na(3)O_5 polyhedra (Figs. S1c, S1d). More details of the structure of $Na_4[UO_2(CO_3)_3]$ have been described previously [5, 8, 9].

3.2 Crystallographic studies

The crystallographic data of typical samples and reference data are listed in Table 1. The unit cells of all synthesized samples are consistent with a single phase. This indicates that the structure of $Na_4[UO_2(CO_3)_3]$ is unaltered subsequent iodine or selenium incorporation into its structure. Similar phenomena have been observed by Klingensmith *et al.* [38] and demonstrated in our previous studies [29, 30].

3.3 Uptake of iodine and selenium by trigonal $Na_4[UO_2(CO_3)_3]$

Similar to our previous studies, a LA-ICP-MS protocol was used to detect the incorporated iodine and selenium

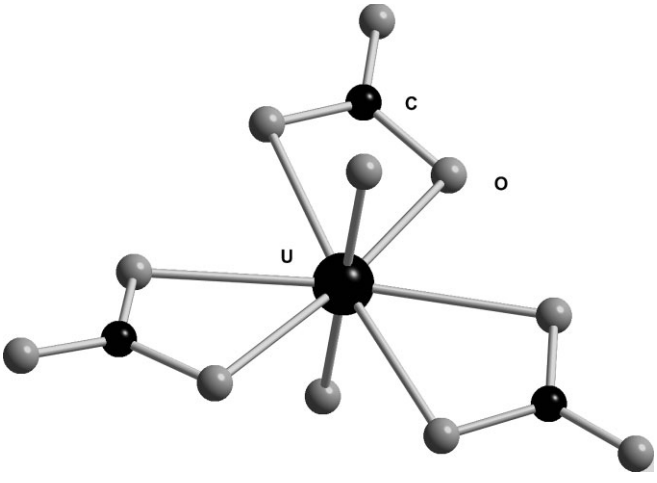

Fig. 1. Schematic model of the uranyl tricarbonate ion $[UO_2(CO_3)_3^{4-}]$.

Table 1. Crystallographic information of trignal $Na_4[UO_2(CO_3)_3]$ and iodine/selenium adopted $Na_4[UO_2(CO_3)_3]$.

Sample	Space group	*a* (Å)	*b* (Å)	*c* (Å)	*α* (°)	*β* (°)	*γ* (°)	References
Douglass	$P\bar{3}c1$	9.32(1)		12.80(1)				11
Li *et al.*	$P\bar{3}c1$	9.3417(7)	9.3417(7)	12.824(1)	90	90	120	8
Císařová *et al.*	$P\bar{3}c1$	9.3380(2)	9.3380(2)	12.8170(3)	90	90	120	9
Ondrus *et al.*	$P1$ or $P\bar{1}$	9.291(2)	9.291(2)	12.895(2)	90.73(2)	90.82(2)	120.00(1)	5
NaUC	$P\bar{3}c1$	9.33	9.33	12.81	90	90	120	This study
NaUCI1a	$P\bar{3}c1$	9.34	9.34	12.82	90	90	120	
NaUCI1b	$P\bar{3}c1$	9.29	9.29	12.61	90	90	120	
NaUCI2a	$P\bar{3}c1$	9.34	9.34	12.82	90	90	120	
NaUCI2b	$P\bar{3}c1$	9.35	9.35	12.71	90	90	120	
NaUCSe1a	$P\bar{3}c1$	9.33	9.33	12.75	90	90	120	
NaUCSe1b	$P\bar{3}c1$	9.34	9.34	12.74	90	90	120	
NaUCSe2a	$P\bar{3}c1$	9.34	9.34	12.82	90	90	120	
NaUCSe2b	$P\bar{3}c1$	9.31	9.31	12.75	90	90	120	

within the synthesized trigonal $Na_4[UO_2(CO_3)_3]$. As shown in Fig. 2, trigonal $Na_4[UO_2(CO_3)_3]$ forms yellow prismatic crystals. Laser ablation experiments were conducted using a ~ 50 μm spot size, which typically resulted in pit depths of ~ 15 μm subsequent ~ 1 min of analysis. Based on the LA-ICP-MS time-resolved spectra shown in Fig. 3, background ion signals are smooth and very low prior to the commencement of lasering. Ion signals (counts per second – cps) for ^{78}Se, ^{127}I and ^{235}U are measured subsequent the onset of lasering, indicating that both iodine and selenium have been incorporated into the crystals of $Na_4[UO_2(CO_3)_3]$. Furthermore, the iodine and selenium ion signals are concomitant with their uranium counterpart as ablation continues from the surface of the crystal towards the interior (Fig. 3). For data reduction purposes, the net ion signals were determined by subtracting the average background ion signals (time interval between 0 and 60 s) from the total ion signals (time interval between 60 and 120 s).

Based on the LA-ICP-MS results (Tables S1 and S2), the molar ratio of I/U in NaUC ranges from 0.000029 to 0.006 for iodate, and from 0.000407 to 0.00603 for periodate; these results indicate therefore that iodine abundances vary from 6.7 to 1300 ppm and 95.4 to 1412 ppm in the form of IO_3^- and IO_4^-, respectively. In contrast, the Se/U ratio in NaUC ranges from 0.000331 to 0.00236 for selenite and from 0.00002 to 0.002 for selenate. This implies that the concentration of incorporated selenium varies between 40 and 391 ppm in the form of SeO_3^{2-}, and between 2.62 and 311 ppm in the form of SeO_4^{2-}.

It is clear that both iodine (IO_3^- and IO_4^-) and selenium (SeO_3^{2-} and SeO_4^{2-}) can be incorporated into the structure of $Na_4[UO_2(CO_3)_3]$ regardless of the different incorporation methods. Iodine and selenium concentrations (ppm) are illustrated in Fig. 4. In total, the abundances of iodine and selenium in U/I(Se) = 10 samples are higher than that in U/I(Se) = 20 samples, which is due to the higher concentration of iodine or selenium in the starting materials. When the same U/I(Se) ratio is used, it is likely that the crystals synthesized in the presence of iodate or selenite (NaUCI1a, NaUCI1b, NaUCSe1a and NaUCSe1b), and thus can uptake more iodine or selenium than pure $Na_4[UO_2(CO_3)_3]$ crystals that reacted with iodate or selenite solution (NaUCI1c, NaUCI1d, NaUCSe1c and NaUCSe1d). However, the opposite trend is observed for periodate and selenate; similar phenomena have also been observed in our previous studies [29, 39]. There are two possible explanations for such differences. One is that the different geometries between iodate and periodate or selenite and selenate result in dif-

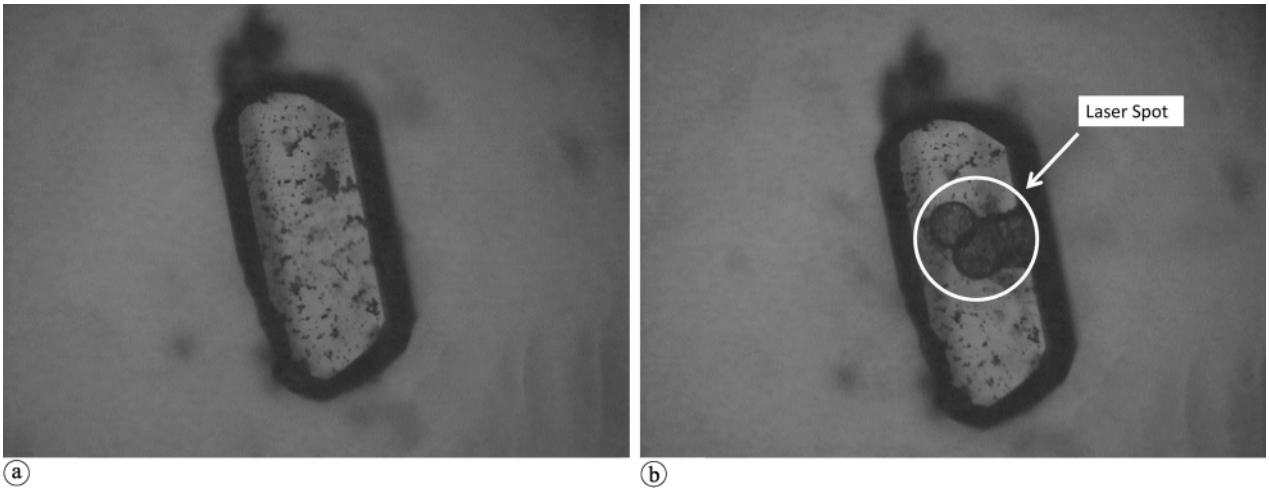

Fig. 2. Photomicrograph of NaUCI2d crystal before (**a**) and after (**b**) laser ablation analysis.

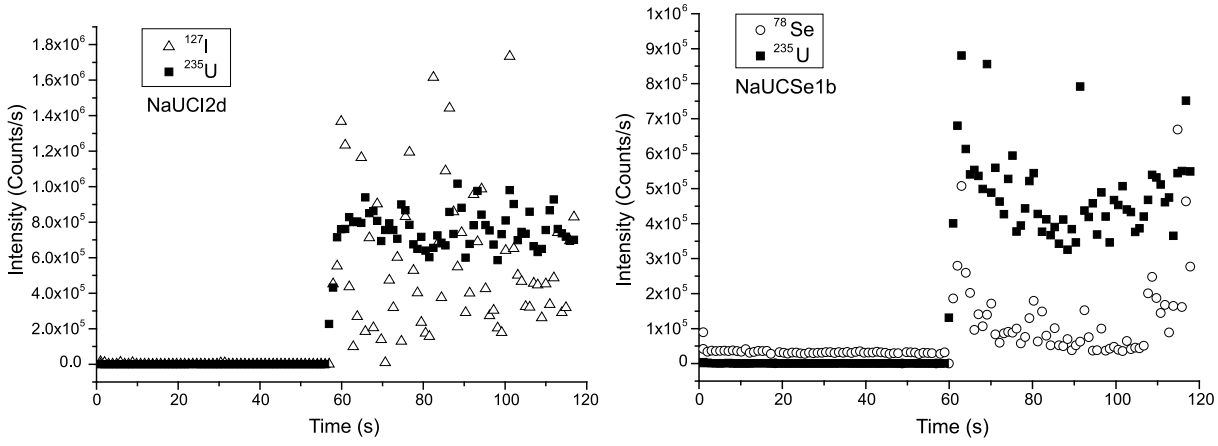

Fig. 3. Typical LA-ICP-MS time-resolved spectra for NaUCl2d and NaUCSe1b.

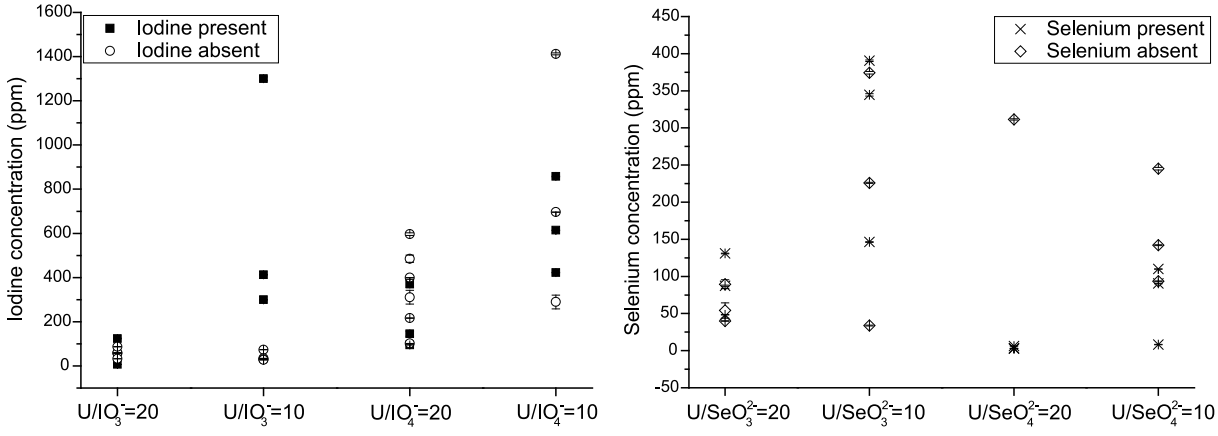

Fig. 4. Concentration of iodine and selenium in the crystals of iodine/selenium adopted $Na_4[UO_2(CO_3)_3]$.

ferent substitution behavior. A second explanation is that these trends are spurious due to the limited data set and the variable distribution of iodine or selenium in the different crystals of the same sample.

3.4 Incorporation mechanisms for iodine and selenium in $Na_4[UO_2(CO_3)_3]$

Generally, anions with similar valences and geometries can easily substitute for one another, such as $SiO_4^{4-} \leftrightarrow PO_4^{3-}$ [31] and $IO_3^- \leftrightarrow HPO_4^{2-}$ [29, 30]. However, Chen *et al.* predicted the possible substitution of $SeO_3^{2-} \leftrightarrow CO_3^{2-}$ in rutherfordine and other uranyl carbonates [27]. Furthermore, the replacement of tetrahedron PO_4^{3-}, SeO_3^{2-} and SeO_4^{2-} by trigonal CO_3^{2-} has been observed [31–37]. Thus, our results indicate that both iodine and selenium can be incorporated into the $Na_4[UO_2(CO_3)_3]$ structure and give credence to the Chen *et al.* hypothesis.

Selenite (SeO_3^{2-}) and selenate (SeO_4^{2-}) have a charge of 2− which is the same as CO_3^{2-}. The substitutions of $SeO_3^{2-} \leftrightarrow CO_3^{2-}$ and $SeO_4^{2-} \leftrightarrow CO_3^{2-}$ in $Na_4[UO_2(CO_3)_3]$ do not require a charge-balance mechanism. These substitutions can be described as Schemes 1 and 2.

$$Na_4[UO_2(CO_3)_3] + xSeO_3^{2-} \rightarrow Na_4[UO_2(CO_3)_{(3-x)}(SeO_3)_x] + xCO_3^{2-} \quad \text{(Scheme 1)}$$

$$Na_4[UO_2(CO_3)_3] + xSeO_4^{2-} \rightarrow Na_4[UO_2(CO_3)_{(3-x)}(SeO_4)_x] + xCO_3^{2-} \quad \text{(Scheme 2)}$$

In contrast, both iodate (IO_3^-) and periodate (IO_4^-) have a charge of 1−, indicating that the substitutions of $IO_3^- \leftrightarrow CO_3^{2-}$ and $IO_4^- \leftrightarrow CO_3^{2-}$ in $Na_4[UO_2(CO_3)_3]$ need a charge-balance mechanism. As shown in Schemes 3 and 4, the most likely possibility is that some sodium cations are lost near the substitution sites, which can supply additional vacancies (□). The vacancy is beneficial for the structure because IO_3^- and IO_4^- tetrahedron are larger than the CO_3^{2-} triangle. This may be the reason why $Na_4[UO_2(CO_3)_3]$ can uptake much more iodine than selenium.

$$Na_4[UO_2(CO_3)_3] + xIO_3^- \rightarrow \square_y Na_{(4-y)}[UO_2(CO_3)_{(3-x)}(IO_3)_x] + xCO_3^{2-} + yNa^+ \quad \text{(Scheme 3)}$$

$$Na_4[UO_2(CO_3)_3] + xIO_4^- \rightarrow \square_y Na_{(4-y)}[UO_2(CO_3)_{(3-x)}(IO_4)_x] + xCO_3^{2-} + yNa^+ \quad \text{(Scheme 4)}$$

Due to the similarity of the B−O and C−O bond lengths, it is of interest to compare the capacity to incorporate iodate into uranyl borates [39] and uranyl carbonate. B−O bond length ranges from 1.36 Å to 1.49 Å, while the C−O bond length varies from 1.28 Å to 1.31 Å. However, the typical length of the I−O and Se−O bonds are 1.80 Å and 1.70 Å, respectively, which are both much longer than the C−O and B−O bonds. According to our previous study, IO_3^- does not substitute for BO_3^{3-} or BO_4^{5-} in uranyl borates because this would disrupt the connectivity of the structure [39].

Table 2. Thermal analyses of trigoanl $Na_4[UO_2(CO_3)_3]$ and iodine/selenium adopted $Na_4[UO_2(CO_3)_3]$.

Sample	Temperature range (°C)	DTA endotherms (°C)	Mass change (%)	Assignment (CO_2)	Total
$Na_4[UO_2(CO_3)_3]$	20–510	393.4	12.09	1.49	2.82
	510–690	681.9	4.20	0.52	
	690–900	805.6	6.56	0.81	
NaUCI1b	20–460	389.0	11.95	1.47	2.79
	460–680	656.6	6.37	0.78	
	680–900	789.6	4.35	0.54	
NaUCI2b	20–425	382.3	10.50	1.29	2.61
	425–670	646.6	5.27	0.65	
	670–900	759.8	5.46	0.67	
NaUCSe1d	20–550	374.0	9.94	1.22	2.49
	550–660	618.2	3.91	0.48	
	660–900	758.8	6.35	0.78	
NaUCSe2d	20–430	377.2	10.82	1.33	2.60
	430–670	629.8	4.41	0.54	
	670–900	777.9	5.85	0.72	

In this study, though the C−O bond length is shorter than B−O bond length, CO_3^{2-} can be substituted by IO_3^- because CO_3^{2-} is isolated from other CO_3^{2-} and not a part of a polymeric anionic network as occurs in borates.

3.5 Thermal gravimetric analysis (TGA)

TG curves of trigonal NaUC and typical iodine or selenium adopted NaUC samples are shown in Fig. S2, while the tentative assignment and interpretation of the TG is given in Table 2. Ondruš *et al.* reported that the major DTA endotherms are at 430, 680, 780, 860, 930, 970 and 455, 785, 855, 930, 960 °C for synthetic Čejkaite and synthetic trigonal $Na_4[UO_2(CO_3)_3]$, respectively [5]. In this study, the DTG endotherms for trigonal NaUC are at 393, 681.9 and 805.6 °C, with the mass changes of 12.09%, 4.20%, 6.56% in the range of 20–510, 510–690 and 690–900 °C. However, after iodine or selenium are incorporated into the structure, the endotherms decreased to lower temperatures. For example, the endotherms for NaUCSe1d are 374.0, 618.2 and 758.8 °C, which are 19, 73.7 and 46.4 °C lower than that of pure $Na_4[UO_2(CO_3)_3]$. The changes of the endotherms are attributed to the incorporation of iodine or selenium, which causes the structure to be less robust, resulting in a lower decomposition temperature. Furthermore, the total mass reduced changed from 22.85% (pure $Na_4[UO_2(CO_3)_3]$) to 22.67%, 21.23%, 20.20%, and 21.08% for NaUCI1b, NaUCI2b, NaUCSe1d, and NaUCSe2d, respectively. These decreases are due to the lower carbon concentration in the iodine- or selenium-bearing samples.

3.6 Environmental implications

There are as many as thirty uranyl carbonate minerals in nature, and almost twenty uranyl carbonate compounds have been synthesized. All of these minerals and compounds have isolated carbonate ligands, indicating that the site of carbonate may be substituted by trace IO_3^-, IO_4^-, SeO_3^{2-} or SeO_4^{2-}. Uraninite and spent fuel is unstable under oxidizing conditions and will change to secondary uranyl minerals, including uranyl carbonates [40–43]. Thus, the migration of ^{129}I and ^{79}Se in uranium ores or repositories should be retarded by the secondary uranyl carbonates *via* this mechanism. In addition, carbonate is ubiquitous in the natural aqueous environment and results in the precipitation of carbonate minerals. For example, calcite ($CaCO_3$) is a very common mineral in surface and sedimentary environments. Previous studies have shown that both SeO_3^{2-} and SeO_4^{2-} can incorporate into calcite by substitution for CO_3^{2-} [34–37]. Considering the similar geometries of IO_3^- and SeO_3^{2-} or IO_4^- and SeO_4^{2-}, it is expected that IO_3^- and IO_4^- may incorporate into calcite by the same mechanism. Since calcite is a common granitic fracture-filling mineral [44, 45], ^{129}I and ^{79}Se released to the far-field of a repository should be co-precipitated with calcite and therefore be immobilized.

Acknowledgment. We are grateful for support provided by the National Natural Science Foundation of China (Grant No. 40972213, 41103055) and the Office of Civilian Radioactive Waste Management, Office of Science and Technology and International, through a subcontract with Argonne National Laboratory (USA).

Appendix available

Details of the LA-ICP-MS results, structure of $Na_4[UO_2(CO_3)_3]$ and TG curves are available in the Appendix.

References

1. Finch, R. J., Murakami, T.: Systematics and paragenesis of uranium minerals. In *Uranium: Mineralogy, Geochemistry and the Environment*. (Burns, P. C., Finch, R. J., eds.) Mineralogical Society of America, Washington DC (1999), pp. 91–179.
2. Clark, D. L., Hobart, D. E., Neu, M. P.: Chem. Rev. **95**(1), 25–48 (1995).
3. Christ, C. L., Clark, J. R., Evans, H. T.: Science **121**(3144), 472–473 (1955).
4. Burns, P. C., Finch, R. J.: Am. Mineral. **84**(9), 1456–1460 (1999).
5. Ondruš, P., Skála, R., Veselovský, F., Sejkora, J., Vitti, C.: Čejkaite. Am. Mineral. **88**(4), 686–693 (2003).
6. Ondruš, P., Veselovský, F., Hlousek, J., Skála, R., Vavrín, I., Fryda, J., Čejka, J., Gabašova, A.: J. Czech Geol. Soc. **42**, 3–76 (1997).
7. Ondruš, P., Veselovský, F., Skála, R., Císarová, L., Hlousek, J., Fryda, J., Vavrín, I., Čejka, J., Gabašova, A.: J. Czech Geol. Soc. **42**, 77–108 (1997).
8. Li, Y., Burns, P. C.: J. Nucl. Mater. **299**(3), 219–226 (2001).

9. Císačová, L., Skála, R., Ondruš, P., Drábek, M.: Acta Crystall. E **57**, i32–i34 (2001).
10. Čejka, J.: Infrared spectroscopy and thermal analysis of the uranyl minerals. In: *Uranium: Mineralogy, Geochemistry and the Environment*. (Burns, P. C., Finch, R., eds.) The Mineralogical Society of America, Washington DC (1999), pp. 521–622.
11. Douglass, R. M.: Anal. Chem. **28**(10), 1635 (1956).
12. FAO & WHO (Food and Agriculture Organization of the United Nations & World Health Organization): Human Vitamin and Mineral Requirements. Rome (2001), pp. 181–194, 235–256.
13. CRWMSM&O (Civilian Radioactive Waste Management System, Management and Operating Contractor): Total System Performance Assessment – 1995: An Evaluation of the Potential Yucca Mountain Repository. B00000000-01717-2200-00136. Rev. 1. TRW Environmental Safety Systems, Inc., Las Vegas, NV (1995).
14. Smith, G. M., Watkins, B. M., Little, R. H., Jones, H. M., Mortimer, A. M.: Biosphere modeling and dose assessment for Yucca Mountain. TR-107190 3294-18. QuantiSci Ltd. (1996).
15. Chakrabrty, S., Bardelli, F., Charlet, L.: Environ. Sci. Technol. **44**(4), 1288–1294 (2010).
16. Shi, K. L., Wang, X. F., Guo, Z. J., Wang, S. G., Wu, W. S.: Colloid Surf. A **349**(1–3), 90–95 (2009).
17. Peitzsch, M., Kremer, D., Kersten, M.: Environ. Sci. Technol. **44**(1), 129–135 (2010).
18. Naveau, A., Monteil-Rivera, F., Guillon, E., Dumonceau, J.: Environ. Sci. Technol. **41**(15), 5376–5382 (2007).
19. Devoy, J., Walcarius, A., Bessiere, J.: Langmuir **18**(22), 8472–8480 (2002).
20. Aldahan, A., Persson, S., Possnert, G., Hou, X. L.: Geophys. Res. Lett. **36**, L11805 (2009).
21. Aldahan, A., Alfimov, V., Possnert, G.: Appl. Geochem. **22**(3), 606–618 (2007).
22. Vance, E. R., Perera, D. S., Moricca, S., Aly, Z., Begg, B. D.: J. Nucl. Mater. **341**(1), 93–96 (2005).
23. Bostock, A. C., Shaw, G., Bell, J. N. B.: J. Environ. Radioactiv. **70**(1–2), 29–42 (2003).
24. Atkins, M., Kindness, A., Glasser, F. P., Gibson, I.: Waste Manage. **10**(4), 303–308 (1990).
25. Hou, X. L., Aldahan, A., Nielsen, S. P., Possnert, G.: Environ. Sci. Technol. **43**(17), 6522–6528 (2009).
26. Reithmeier, H., Lazarev, V., Ruhm, W., Schwikowski, M., Gäggeler, H. W., Nolte, E.: Environ. Sci. Technol. **40**(19), 5891–5896 (2006).
27. Chen, F. R., Burns, P. C., Ewing, R. C.: J. Nucl. Mater. **275**(1), 81–94 (1999).
28. Wu, S. J., Chen, F. R., Kang, M. L., Yang, Y. Q., Dou, S. M.: Radiochim. Acta **97**(8), 459–465 (2009).
29. Ling, J., Wu, S. J., Chen, F. R., Simonetti, A., Shafer, J. T., Albrecht-Schmittt, T. E.: Inorg. Chem. **48**(23), 10995–11001 (2009).
30. Wu, S. J., Chen, F. R., Simonetti, A., Albrecht-Schmitt, T. E.: Environ. Sci. Technol. **44**(8), 3192–3196 (2010).
31. Pan, Y., Fleet, M. E.: Compositions of the apatite-group minerals: substitution mechanisms and controlling factors. Rev. Mineral. Geochem. **48**(1), 13–49 (2002).
32. Comodi, P., Liu, Y.: Eur. J. Mineral. **12**(5), 965–974 (2000).
33. Tacker, R. C.: Am. Mineral. **93**(1), 168–176 (2008).
34. Lamble, G. M., Lee, J. F., Staudt, W. J., Reeder, R. J.: Physica B **208**–**209**, 589–590 (1995).
35. Aurelio, G., Fernández-Martínez, A., Cuello, G. J., Román-Ross, G., Alliot, I., Charlet, L.: Chem. Geol. **270**(1–4), 249–256 (2010).
36. Reeder, R. J., Lamble, G. M., Lee, J.-F., Staudt, W. J.: Geochim. Cosmochim. Acta **58**(24), 5639–5646 (1994).
37. Staudt, W. J., Reeder, R. J., Schoonen, M. A. A.: Geochim. Cosmochim. Ac. **58**(9), 2087–2098 (1994).
38. Klingensmith, A. L., Deely, K. M., Kinman, W. S., Kelly, V., Burns, P. C.: Am. Mineral. **92**(4), 662–669 (2007).
39. Wu, S. J., Wang, S. A., Simonetti, A., Chen, F. R., Albrecht-Schmitt, T. E.: Radiochim. Acta **99**(9), 573–579 (2011).
40. Wronkiewicz, D. J., Bates, J. K., Gerding, T. J., Veleckis, E., Tani, B. S.: J. Nucl. Mater. **190**, 107–127 (1992).
41. Finch, R. J., Ewing, R. C.: J. Nucl. Mater. **190**, 133–156 (1992).
42. Deditius, A. P., Utsunomiya, S., Ewing, R. C.: J. Alloy. Compd. **444**, 584–589 (2007).
43. Wronkiewicz, D. J., Bates, J. K., Wolf, S. F., Buck, E. C.: J. Nucl. Mater. **238**(1), 78–95 (1996).
44. Ticknor, K., Cho, Y.: J. Radioanal. Nucl. Chem. **140**(1), 75–90 (1990).
45. Whelan, J. F., Paces, J. B., Peterman, Z. E.: Appl. Geochem. **17**(6), 735–750 (2002).